ISTITUTO NAZIONALE DI FISICA NUCLEARE

Sezione di Bari

INFN/AE-96/17
10 Giugno 1996

R. Bellotti, M. Boezio, M. Castellano, C. De Marzo, P. Picozza, V. Prigiobbe,
R. Sparvoli, M. Tirocchi:

COSMIC RAY ANTIPROTON/ELECTRON DISCRIMINATION CAPABILITY OF THE CAPRICE SILICON-TUNGSTEN CALORIMETER NETWORKS

Submitted to *Nuclear Instruments & Methods in Physics Research*

PACS: 95.55.Vj, 29.40.Vj, 84.35
Keywords: cosmic ray, antiproton identification, calorimeter, neural network

SIS-Pubblicazioni
dei Laboratori Nazionali di Frascati

INFN – Istituto Nazionale di Fisica Nucelare
Sezione di Bari

INFN/AE–96/17
10 Giugno 1996

COSMIC RAY ANTIPROTON/ELECTRON DISCRIMINATION CAPABILITY OF THE CAPRICE SILICON–TUNGSTEN CALORIMETER USING NEURAL NETWORKS

R. Bellotti[1(*)], M. Boezio[2], M. Castellano[1(*)], C. De Marzo[1], P. Picozza[3], V. Prigiobbe[3], R. Sparvoli[3], M. Tirocchi[3]

[1] INFN and Università di Bari, Via Amendola 173, I–70126 Bari, Italy
[2] INFN and Università di Trieste, Via Padriciano 99, I–34012 Trieste, Italy
[3] INFN and Università di Roma "Tor Vergata", Via della Ricerca Scientifica 1, I–00133 Roma, Italy

Abstract

A data analysis based on an artificial neural network classifier is proposed to identify cosmic ray antiprotons detected with the CAPRICE silicon-tungsten imaging calorimeter against electron background in the energy range 1.2-4.0 GeV. A set of new physical variables, describing the events inside the calorimeter on the base of their different patterns, are introduced in order to discriminate between hadronic and electomagnetic showers. The ability of the artificial neural network classifier to perform a careful multidimensional analysis gives the possibility to identify antiprotons with an electron rejection 408 ± 85(stat) at 95.0 ± 0.2 (stat)% of signal detection efficiency. The high accuracy achieved by this method improves substantially the efficiency in the evaluation of the cosmic ray antiproton spectrum.

* Corresponding Authors: Phone 39–80–5443173
e–mail: Bellotti@ba.infn.it – Castellano@ba.infn.it

1 Introduction

The study of cosmic ray antiprotons ($\bar{p}$) is of fundamental astrophysical interest. Detailed measurements of the $\bar{p}$ energy spectrum provide a crucial test of models describing $\bar{p}$ origin and propagation in the interstellar medium [1]. Since their discovery in 1979, by two independent balloon-borne experiments [2, 3], the cosmic ray $\bar{p}$ measurement remains a difficult experimental task [4]. The energy region explored so far, which spans the interval from 0.2 to 20 GeV approximately, is limited and the statistical significance of the flux and $\bar{p}/p$ ratio needs futher improvements.

The CAPRICE balloon-borne experiment [5] has been devoted to measure the flux of low-energy antiprotons, positrons and light isotopes in the cosmic radiation. It was flown by a stratospheric balloon on 8-9 august 1994 over northen Canada and it collected data during more than 21 hours at a floating altitude less than 5 g/cm^2. The detector system employed is shown in fig. 1. It consists of: (1) a superconducting magnet, equipped with multiwire proportional chambers and drift chambers, used as spectrometer; (2) a set of plastic scintillators providing trigger, time-of-flight and absolute charge measurements; (3) a Ring Imaging Cherenkov (RICH) as a β selector and (4) a silicon-tungsten imaging calorimeter to identify different particles according to the topological and energetic patterns of their interactions.

Nowadays many procedures currently used in high energy physics - from off-line data analysis [6] to real time pattern recognition (triggering) [7] - are performed applying neural network (NN) techniques. NNs are particularly apt to classify complex phenomena and provide robust and reliable methods to design efficient and fast systems for particle identification systems.

In this paper we study the $\bar{p}$/electron discrimination capability of the CAPRICE silicon-tungsten calorimeter [8], by means of a neural network classifier, with the task to improve the CAPRICE $\bar{p}$ statistics. The limited depth of the calorimeter is insufficient for the full containment of the high energy electromagnetic showers (background events), neverthless the high granularity and the energy resolution of the calorimeter silicon wafers make them capable to measure the lateral and longitudinal shower profiles. In order to carefully describe the difference between hadronic and electromagnetic showers, several discriminating variables have been introduced. The ability of NN algorithms to perform a careful multidimensional analysis allows to take into account a large number of discriminating variables in order to exploit the difference between hadronic and electromagnetic showers. As a result a very high antiproton identification efficiency has been achieved.

2 Discriminating variables

The CAPRICE silicon-tungsten calorimeter, positioned at the bottom of the balloon payload, is composed of 8 silicon planes, sensitive both in the X and Y coordinates, each interleaved with one radiation lenght (=3.5 mm) of tungsten, for a total calorimeter thickness of seven radiation lengths. The sampling layer of the calorimeter is an array of 8 x 8 pairs (X-Y) of detectors (6 x 6 cm^2, divided in 16 strips, each 3.6 mm wide). Each sampling layer consists of two arrays having 128+128 readout channels. A built-in system equipped with ADCs and digital processors accomplishes the data acquisition.

An electromagnetic shower developing in tungsten consists of a cascade of photons producing $e^{\pm}$ pairs producing photons in turn. Due to the pair production threshold of order a few MeV, even photons or electrons of energy quite less than 1 GeV can initiate such a shower. As a rule, all massive particles in the e.m. shower ($e^{\pm}$) are relativistic and the general shape of the shower volume is a well defined cone with vertex in the first interaction point and a small aperture angle. The transversal development of an e.m. shower is quite regular and is well described by the Molière theory: the 99% of an e.m. shower, at any energy, is contained in a cylindrus of ratio R=3,5 RM, where RM is the Molière radius whose value is fixed for each material (0.69 cm for tungsten). Quite different is the behaviour of the particles inside a hadronic shower, usually initiated by a proton or an antiproton. Here the cascade is mainly due to strong interactions with tungsten nuclei; its volume is not so well defined and secondary particles at large angles may be present.

In the CAPRICE calorimeter the $\bar{p}$/electron recognition is achieved by exploiting the different longitudinal and lateral energy deposit profile of electromagnetic and hadronic showers. To this end, some discriminating variables have been defined for the detected events describing their energy and the number of hits along with other information on the shower development patterns.

These variables are as follows:

(1) The total energy released in the whole calorimeter.

(2) The total number of fired strips in the whole calorimeter.

(3) The total number of fired strips inside a cylinder of radius equal to 4 Molière radii, around the track direction.

(4) The total number of fired strips inside a cylinder of radius equal to 1 Molière radius, around the track direction.

(5) The total energy released in a cylinder of radius equal to 1 Molière radius, around the track direction.

(6) The maximum energy released in a single strip in the whole calorimeter.

(7) The total energy released in the two plane of maximun interaction, i.e. having the higher energy deposit.
(8) The medium distance between the most separated fired strips in each plane.

Even though other possible variables could be introduced, our experience and the results here presented show that the 8 variables defined above rappresent a set particularly good for a multidimensional analysis of the event patterns in the CAPRICE calorimeter.

3 Experimental results

3.1 The simulated data sets

To evaluate the $\bar{p}$/electron discrimination capability of the CAPRICE calorimeter, using the set of discriminating variables above introduced and the NN classifier described below, the detector has been simulated using the GEANT code [9]. In order to reproduce the physical situation of the detector in the payload and in order to take into account all passive materials crossed by the particles, we simulated: a) the aluminium box (2 mm), embedding the whole silicon detector; b) the plexiglass layer (2 cm), placed at the top of the apparatus in order to protect the first silicon plane; c) the real silicon-tungsten detector.

The calorimeter response has been studied for electrons and antiprotons at momenta of 1.2, 1.6, 2.0, 2.1, 2.6, 3.0, 3.1, 3.6, 4.0 GeV/c; particles (samples of 1000 events for each energy) hit the calorimeter orthogonally, at the center of the first plane. After a number of optimisations, the GEANT energy cut has been fixed at 10 keV; this means that GEANT follows a secondary particle until its energy is above or equal this value, then drops it out. For each active silicon strip, a threshold corresponding to an energy of 0.7 mips (minimum ionising particle energy, fixed to 95 keV) has been imposed to reproduce the real data analysis procedure that separates the noise of the electronics from the signal and eliminates it.

3.2 The NN classifier

For the multidimensional analysis of the calorimeter events a "three-layered feed-forward" Neural Network has been considered [10]. It consists of units (formal neurons) arranged in contiguous layers, as shown in fig. 2. Each neuron k ($k = 1, \ldots, N_h$) belonging to the hidden layer receives as input the output X_l ($l = 1, \ldots, N_i$) of all the l neurons of the input layer, to which it is connected by $w_{lk}^{(1)}$ synaptic strengths. On the other hand, the neuron k is also connected, with strengths $w_{ki}^{(2)}$, to the neuron of the output layer. The transfer function of the neurons is the sigmoid funtion:

$$g(x,\theta) = \frac{1}{1+\exp(-\beta(x-\theta))} \quad (1)$$

where θ and β are the neuron threshold and the gain factor, respectively.

The synaptic matrix $W^{(old)}$ is trained by showing to the network a data set of examples (training data set) and updating the weights according to the delta rule, which minimizes the mean squared error function E of the classification system [10]. After each training epoch, the quality of the new model $W^{(new)}$ is estimated by means of an independent data set (test data set). The learning session is stopped when the error function E, evaluated on the test set, reaches its lowest value. The training and stopping procedures are unbiased general criteria to build up a classification system in an accurate way. Tables 1 summarizes the parameters for the NN classifier used in this paper.

Table 1. Characteristics of the neural network used to classify the calorimeter data.

Neurons in the input layer	9
Neurons in the hidden layer	5
Neurons in the output layer	1
β gain factor	1
θ neuron threshold	0.5
α momentum term	0.9
η learning rate	1
Learning algorithm	Backpropagation
Learning mode	Incremental
Number of Epochs	900
Training Set Cardinality	4500
Test Set Cardinality	4500

From the point of view of data analysis each input neuron is associated with a physical variable. Therefore the NN enables one to explore a multidimensional input space by taking into account several complex information about the physical event. The set of discriminating variables introduced are fed to the artificial NN described in table 1 together with the rigidity of the event measured by the spectrometer. Moreover this procedure enables to correlate automatically the rigidity of the particle with the different behaviour of the discriminating variables in different parts of the energy spectrum.

For the purpose of evaluating the discrimination capability of the CAPRICE calorimeter its performance has been investigated in simulation using the multidimensional classifier above described. Performance indicators are obtained evaluating the relative electron rejection $\rho = N_e/n_{e\bar{p}}$ versus the antiproton efficiency $\epsilon = n_{\bar{p}\bar{p}}/N_{\bar{p}}$; where:

$n_{e\bar{p}}$ and $n_{\bar{p}\bar{p}}$ are the number of electrons misclassified as antiprotons and the number of antiprotons correctly classified, respectively;
N_e and $N_{\bar{p}}$ are the total number of electrons and antiprotons in the simulated data set.

A critical step has been to find the best NN architecture, where the number of hidden neurons is considered optimal when it is large enough to ensure a high degree of classification and small enough to ensure a high degree of generalization. The experimental evidence on the independent test set has shown that the best performance are obtained with five hidden neurons, even though a difference of a few percent only is obtained using a number of hidden neurons ranging from 3 to 20. The feature spaces for background (electron) and signal (antiproton) events are shown in figs. 3 and 4. The electron rejection as a function of antiproton efficiency is shown in fig. 5. This result is one order of magnitude better than those achived by means of mono- and bi-dimensional cuts on the chosen discriminating variables [8].

4 Conclusions

In this paper a classification system based on a neural network is proposed to identify antiprotons detected by the CAPRICE calorimeter. Results show that the neural network classifier is capable of discriminating between antiprotons and electrons with very high efficiency. Specifically, the data analysis method here proposed permits to identify antiprotons with an electron background rejection of 408 $\pm$ 85(stat) at the efficiency of 95.0 $\pm$ 0.2 (stat)%. This result is particularly useful in the context of balloon-borne experiments where, in searching rare events with the constraint of short exposure time, a detection efficiency as large as possible is required. The neural network based analysis presented here will be used to improve the evaluation of the energy spectra of cosmic ray antiprotons in the CAPRICE experiment.

Acknowledgements

This article has been made possible by our participation in the WIZARD Collaboration, which we are glad to thank. We like to thank also Mr. P. Mastrototaro for his collaboration on numerical analysis.

References

[1] S.A. Stephens and R.L. Golden, Space Science Rev. **46** (1987) 31.

[2] R.L. Golden et al., Phys. Rev. Lett. **43** (1979) 1264.

[3] E.A. Bogomolov et al., Proc. of 16th International Cosmic Ray Conference, **1** (1979) 330.

[4] C. N. De Marzo, "Antiproton measurements and antinuclei search", Proc. of Workshop on Frontier objects in astrophysics and particle physics; Vulcano, Italy, june 1996, in press.

[5] R.L. Golden et al., Proposal to NASA NRA-92-OSSA-10.

[6] Delphi Coll., Phys. Lett. B **295** (1992) 383.

L3 Coll., Phys. Lett. B **307** (1993) 237.

Aleph Coll., Phys. Lett. B **313** (1993) 549.

Wizard-TS93 Coll., to appear in Astroparticle Physics, Int. Rep. LNF-95/046.

[7] C.S. Lindsey et al., Nucl. Instr. and Meth. A **317** (1992) 346.

B. Denby et al., Nucl. Instr. and Meth. A. **356** (1995) 485.

C. Baldanza et al., Nucl. Instr. and Meth. A. **361** (1995) 506.

[8] M. Bocciolini et al., Nucl. Instr. and Meth. A **370** (1996) 403.

[9] Brun et al., Detector description and simulation tool, CERN program library.

[10] J. Hertz, A. Krogh and R.G. Palmer, Introduction to the Theory of the Neural Computation, Addison-Wesley, (1991).

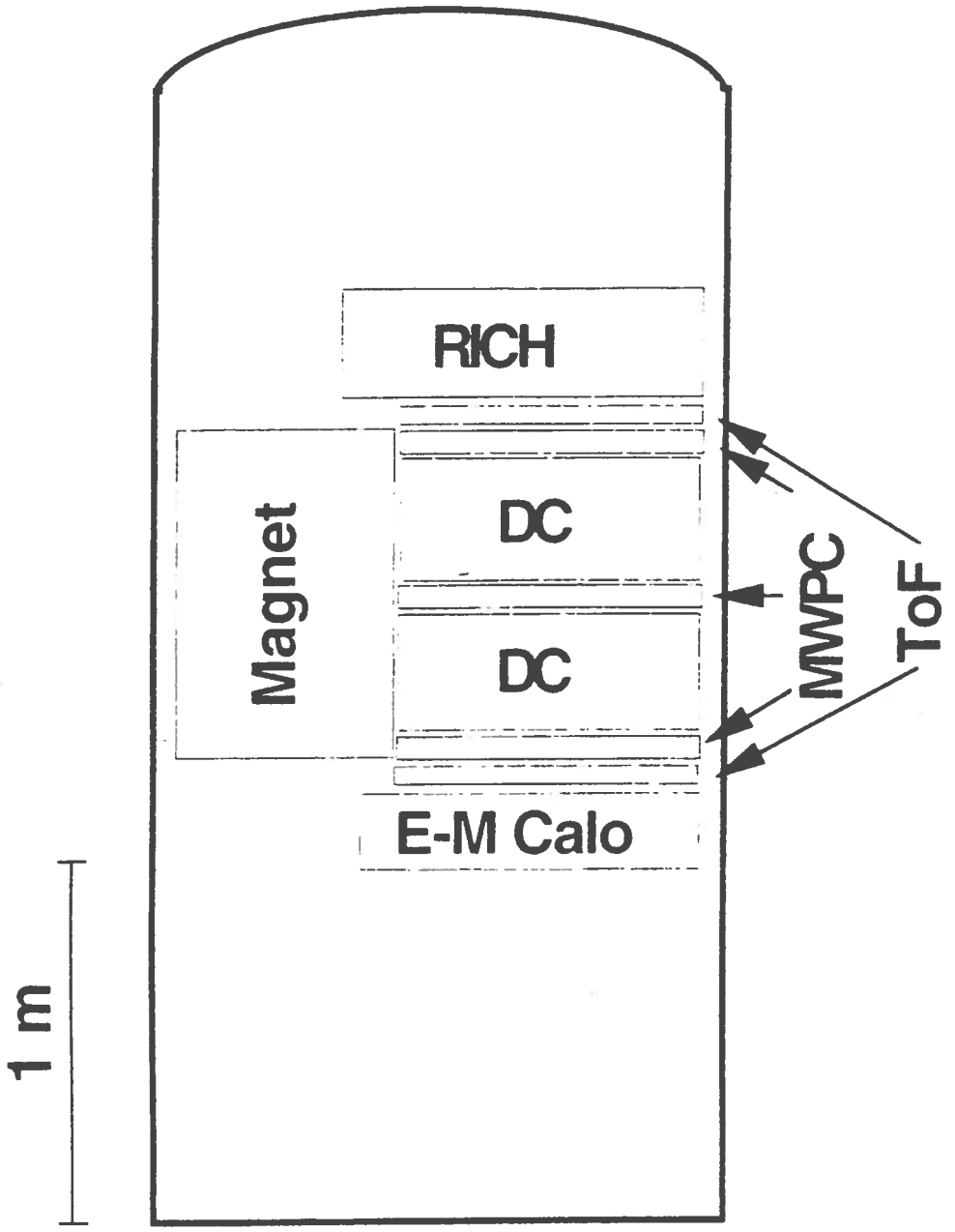

Fig. 1. Schematic diagram of the Wizard-CAPRICE apparatus used for the 1994 balloon flight to identify low energy cosmic ray antiprotons

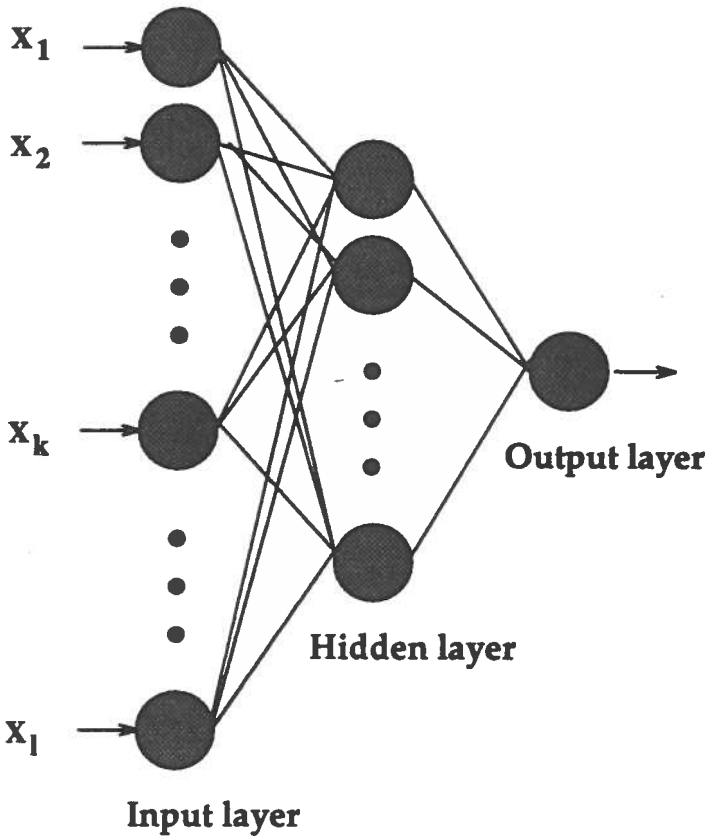

Fig. 2. The three-layered feed-forward neural network classifier used to select antiprotons with the CAPRICE silicon-tungsten calorimeter.

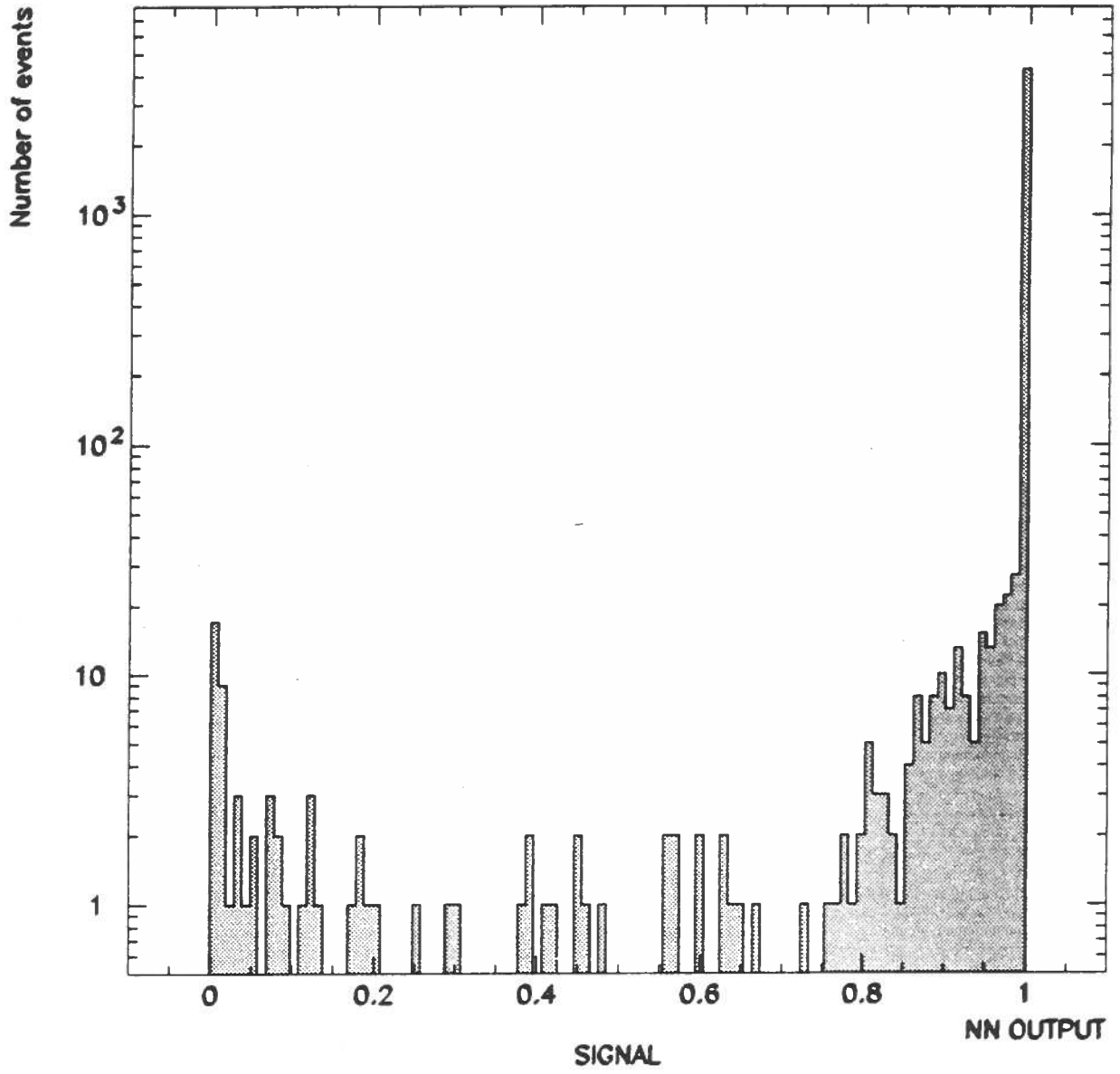

Fig. 3. The neural network output for calorimeter signal events.

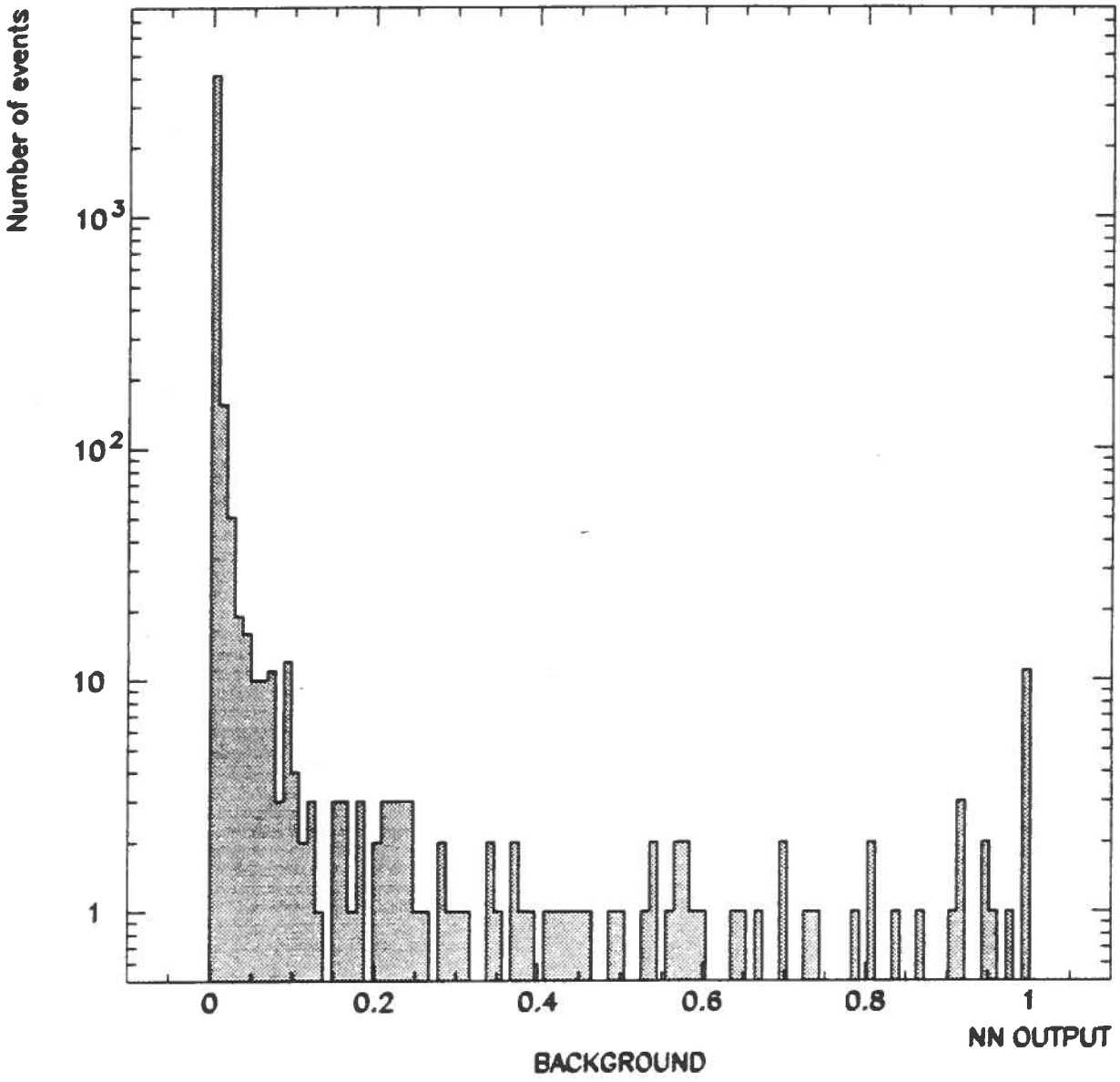

Fig. 4. The neural network output for calorimeter background events.

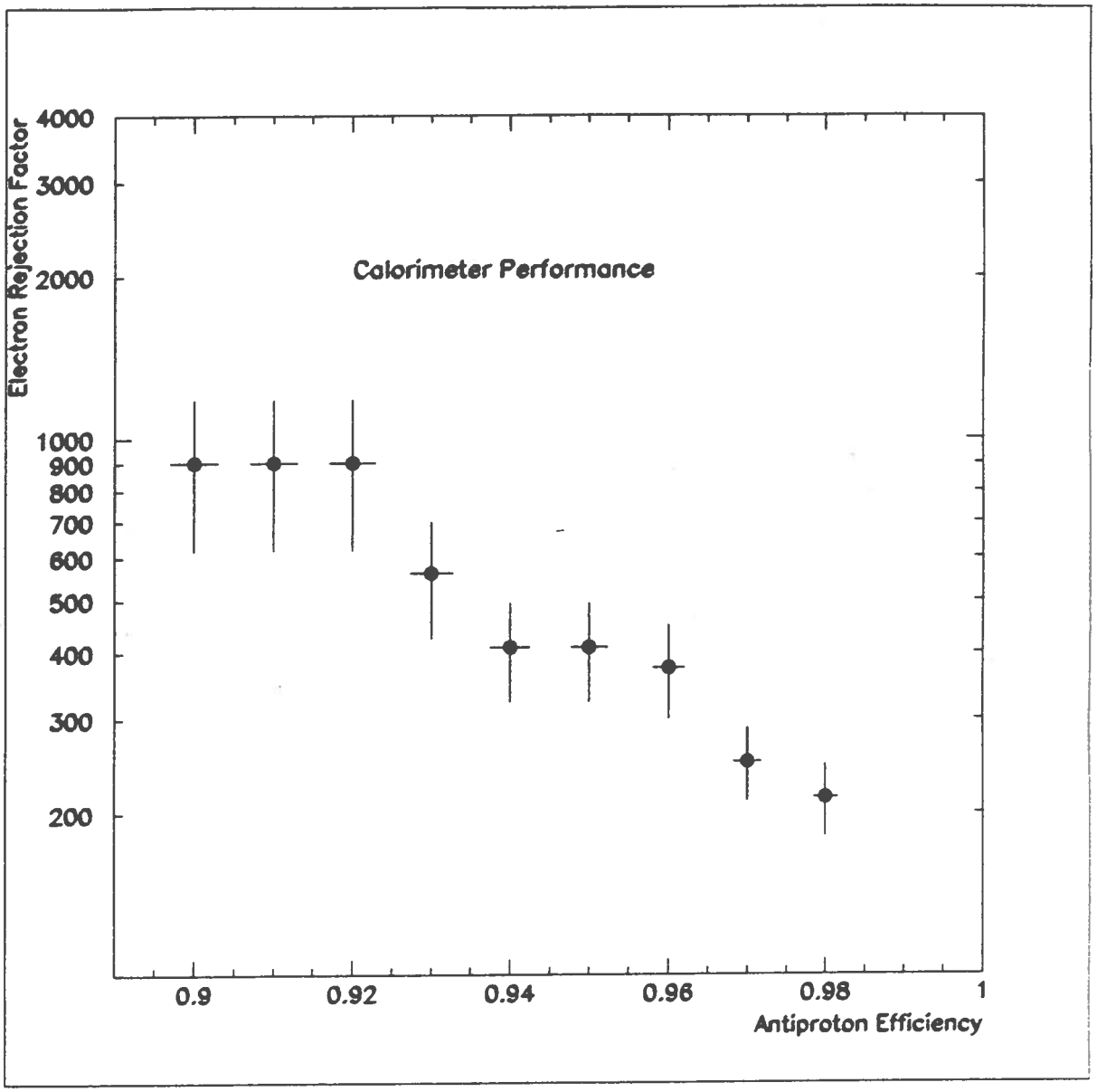

Fig. 5. Electron rejection factor versus antiproton signal efficiency.